

Structural, electronic and magnetic properties of the metal squarate tetrahydrate polymers $\text{Fe}(\text{C}_4\text{O}_4) \cdot 4\text{H}_2\text{O}$ and $\text{Cu}(\text{C}_4\text{O}_4) \cdot 4\text{H}_2\text{O}$

G. M. Frankenbach*, M. A. Beno, A. M. Kini, J. M. Williams**, U. Welp,
J. E. Thompson

Chemistry and Materials Science Division, Argonne National Laboratory, 9700 Cass Avenue, Argonne, IL 60349-4831 (USA)

and M.-H. Whangbo**

Department of Chemistry, North Carolina State University, Raleigh, NC 27695-8204 (USA)

(Received July 16, 1991; revised October 18, 1991)

Abstract

Iron(II) squarate tetrahydrate (**1**), $M_r = 239.95$, $\text{Fe}(\text{C}_4\text{O}_4) \cdot 4\text{H}_2\text{O}$, crystallizes having a monoclinic space group = $C2/c$, $a = 9.066(3)$, $b = 13.417(3)$, $c = 6.777(2)$ Å, $\beta = 98.77(2)^\circ$, $V = 814.8(4)$ Å³, $Z = 4$, $D_x = 1.956(1)$ g cm⁻³, $\lambda(\text{Mo K}\alpha) = 0.71073$, $\mu = 18.613$ cm⁻¹, $F(000) = 488$, $T = 300$ K, $R = 0.025$, $R_w = 0.028$, for 687 observed reflections with $|F_o| > 0$. Copper(II) squarate tetrahydrate (**2**), $M_r = 247.65$, $\text{Cu}(\text{C}_4\text{O}_4) \cdot 4\text{H}_2\text{O}$, crystallizes having a monoclinic space group = $P2_1/c$, $a = 6.676(2)$, $b = 7.946(4)$, $c = 7.688(2)$ Å, $\beta = 110.39(2)^\circ$, $V = 381.4(3)$ Å³, $Z = 2$, $D_x = 2.157(2)$ g cm⁻³, $\lambda(\text{Mo K}\alpha) = 0.71073$ Å, $\mu = 28.833$ cm⁻¹, $F(000) = 250$, $T = 300$ K, $R = 0.025$, $R_w = 0.028$, for 627 observed reflections with $|F_o| > 0$. Extended Hückel molecular orbital (EHMO) calculations on model clusters, $[\text{Fe}(\text{OH})_4(\text{C}_4\text{O}_4)_2]^{6-}$ and $[\text{Cu}(\text{OH})_4(\text{C}_4\text{O}_4)_2]^{6-}$, indicate that **1** and **2** are not good candidates for polymeric electrical conduction, because overlap between the metal and the squarate orbitals is negligible in the HOMO and LUMO of the model clusters. In addition, EHMO calculations suggest that the electronic forces cannot account for the structural differences found between **1** and **2**. The magnetic susceptibility of **2**, measured as a function of temperature, suggests that magnetic spins do not interact via the squarate anion bridges.

Introduction

Several transition metal squarate[†] tetrahydrate salts, $\text{M}(\text{C}_4\text{O}_4) \cdot 4\text{H}_2\text{O}$, with divalent metal ions ($\text{M} = \text{Mn}, \text{Fe}, \text{Co}, \text{Ni}$ and Zn) are known [1]. These divalent tetrahydrate salts are reported to be isotypic. Their structures consist of one-dimensional metal squarate chains interlinked by hydrogen bonding. Contrary to earlier expectations, based on similar compounds formed with the croconate ligand [1], squarate does not act as a chelating ligand in any of these complexes^{††}.

The divalent metal squarate tetrahydrate series could be possible precursors to low dimensional polymeric electrical conductors or molecular magnets, because the linear metal squarate chains would appear to serve as a pathway for electron conduction or magnetic

superexchange. As with other one-dimensional conductors [3], it was expected that the metal squarate tetrahydrates might become good electrical conductors upon partial oxidation or reduction. We chose to study $\text{Fe}(\text{C}_4\text{O}_4) \cdot 4\text{H}_2\text{O}$ (**1**) because iron(II) salts are easily oxidized, and $\text{Cu}(\text{C}_4\text{O}_4) \cdot 4\text{H}_2\text{O}$ (**2**) because numerous copper oxide compounds have been found to be metals and superconductors [4].

To judge the potential of these materials as possible conducting polymers, we determined the structures of **1** and **2** and then used these structural data to perform extended Hückel molecular orbital (EHMO) calculations [5]. These calculations have previously been shown to provide details of metal–ligand bonding which are useful in predicting the conductivity behaviors of partially oxidized or reduced compounds [6].

Low-temperature ordering of magnetic dipoles occurs in squaric acid [7] and some of its salts [8]. Therefore, we performed magnetic measurements of **2** to characterize the state of the copper(II) ion and the interactions between the copper(II) ions.

*Current address. The Procter and Gamble Co., Miami Valley Laboratories, P. O. Box 398707, Cincinnati, OH 45239-8707, USA.

**Authors to whom correspondence should be addressed.

[†]The common name for the dianion of 3,4-dihydroxy-3-cyclobutene-1,2-dione.

^{††}Squarate has been found to act as a chelating ligand only with very large ions such as cerium [2].

Experimental

Brilliant yellow needles of **1** were grown by slow evaporation at room temperature of an equimolar solution of iron(II) sulfate heptahydrate and squaric acid in distilled water. When exposed to air, **1** became brown and cloudy indicating oxidation of iron(II) to iron(III) while retaining its color and brilliance when stored under N₂. *Anal.* Calc. for Fe(C₄O₄)·4H₂O (**1**): C, 20.02; H, 3.26; O, 53.34. Found: C, 20.33; H, 3.26; O, 53.75%.

Brilliant green blocks of **2** were grown at 5 °C from an equimolar solution of copper(II) nitrate trihydrate and squaric acid in distilled water. At room temperature, **2** decomposed due presumably to dehydration but retained its color and brilliance when stored at 5 °C. *Anal.* Calc. for (C₄O₄)·4H₂O (**2**): C, 19.40; H, 3.26; O, 51.69. Found: C, 19.29; H, 3.19; O, 48.89%. Elemental analyses were performed by Midwest Microlab, Indianapolis, IN.

The samples used for X-ray diffraction data collection included a needle of **1** having the dimensions 0.1 × 0.1 × 0.3 mm and a plate of **2** having the dimensions 0.07 × 0.15 × 0.22 mm. The X-ray diffraction data were collected on Nicolet P2₁ automated diffractometer using Mo K α radiation. Unit cell dimensions were obtained from a least-squares analysis of 25 reflections in the angular range 10 < 2 θ < 20°. Intensity data were collected using θ -2 θ scans with variable scan speeds of 2 to 12° min⁻¹, to $\sin\theta/\lambda = 0.59$ for both compounds. Three standard reflections measured every 100 reflections showed < 2% intensity variation. Data were corrected for Lorentzian and polarization effects, and multiple

measured reflections (standards and 0*kl* zone) were averaged. Details of data collection and refinement are given in Table 1. The structures were solved by use of MULTAN78 [9] and Fourier methods. The function minimized was $\sum w(|F_o| - |F_c|)^2$, where $w = 1/\sigma^2(F_o)$ and $\sigma(F_o) = [\sigma^2(F_o^2) + (0.02F_o^2)^2]^{1/2}/2F_o$, with the value of $\sigma(F_o^2)$ based on counting statistics. Atomic scattering factors including anomalous contributions were taken from the International Tables for X-ray Crystallography [10]. All calculations were done by use of a local modification of the UCLA Crystallographic Package [11]. Hydrogen atoms were included at positions observed in Fourier maps with $B_{\text{iso}} = 3.5 \text{ \AA}^2$. All non-hydrogen atoms were refined with anisotropic temperature factors $\Delta/\sigma \leq 0.05$ in the final least-squares cycle resulting in the agreement factors given in Table 1.

In the EHMO calculations, the simple clusters [Fe(OH)₄(C₄O₄)₂]⁶⁻ and [Cu(OH)₄(C₄O₄)₂]⁶⁻ were used to model the iron(II) coordinate environment of **1** and the copper(II) coordinate environment of **2**, respectively. In these model compounds, the M-O-H (M = Fe, Cu) linkages were taken to be linear, and all the M-O bond lengths were taken to be identical to the corresponding ones in **1** and **2**. In constructing the model clusters, we employ OH⁻ instead of H₂O for the purpose of simplicity. However, the essence of our calculational results is not affected by this approximation.

Magnetic susceptibility of a 4.4 mg sample of **2**, composed of non-oriented crystallites, was measured in a commercial SQUID magnetometer. The field

TABLE 1. Crystal structure parameters and data collection

	Fe(C ₄ O ₄)·4H ₂ O (1)	Cu(C ₄ O ₄)·4H ₂ O (2)
Space group	C2/c	P2 ₁ /c
<i>a</i> (Å)	9.066(3)	6.676(2)
<i>b</i> (Å)	13.417(2)	7.946(4)
<i>c</i> (Å)	6.777(2)	7.668(2)
β (°)	98.77(2)	110.39(2)
<i>V</i> (Å ³)	814.8(4)	381.4(3)
<i>Z</i>	4	2
<i>F</i> (000)	488	250
<i>D</i> _{calc} (g cm ⁻³)	1.956(1)	2.157(2)
μ (cm ⁻¹)	18.613	28.833
No. reflections collected	2006	816
No. unique, non-extinct reflections	712	666
No. reflections with $ F_o > 0$	687	627
Refined parameters	61	61
	-10 ≤ <i>h</i> ≤ 0	0 ≤ <i>h</i> ≤ 7
	-14 ≤ <i>k</i> ≤ 14	0 ≤ <i>k</i> ≤ 9
	0 ≤ <i>l</i> ≤ 7	-8 ≤ <i>l</i> ≤ 8
<i>R</i> _{av}	0.022	0.020
<i>R</i> (<i>F</i> _o)	0.025	0.039
<i>R</i> _w (<i>F</i> _o ²)	0.028	0.034
<i>GOF</i>	1.40	2.04

strength was 500 Oe and the temperature range was 5 to 300 K.

Results

A comparison of the unit cell parameters and crystal structure data for **1** and **2** is given in Table 1. Only compound **2** was found to be isostructural with a known series of transition-metal squarate tetrahydrates [1]. The X-ray crystal structure of $\text{Zn}(\text{C}_4\text{O}_4) \cdot 4\text{H}_2\text{O}$ (**3**), a member of an isostructural series, has been reported (with $C2$ as the space group) [1]. When the space group choice is ambiguous, it is conventional to use the centric setting. After collection of X-ray diffraction data from **1**, we found that the intensity statistics indicated the centric space group $C2/c$. The R factor for **1**, $R_w = 0.028$, is much lower than that found for **3**, $R_w = 0.061$, further supporting the centric assignment.

The atom labeling schemes of **1** and **2** are given in Fig. 1(a) and (b), respectively. Tables 2 and 3 contain the final atomic positional parameters of **1** and **2**, respectively. Tables 4 and 5 contain the bond lengths and bond angles of **1** and **2**, respectively.

In **1**, iron(II) is coordinated to the p_σ -orbital of the squarate oxygen atom as shown by the torsion angle $\text{C}(2)\text{--}\text{C}(1)\text{--}\text{O}(1)\text{--}\text{Fe}(1) = 3.4^\circ$. The environment around iron(II) is a slightly distorted octahedron. The iron(II) to the squarate oxygen bond length, $\text{Fe}(1)\text{--}\text{O}(1) = 2.115(2) \text{ \AA}$, is comparable to iron to water oxygen bond length, $\text{Fe}(1)\text{--}\text{O}(3) = 2.151(2)$ and

TABLE 2. Non-H-atom parameters and equivalent isotropic thermal parameters (\AA^2) with e.s.d.s in parentheses for the structure of $\text{Fe}(\text{C}_4\text{O}_4) \cdot 4\text{H}_2\text{O}$ (**1**)

Atom	x	y	z	$U_{\text{eq}} \times 10^5$
Fe(1)	0.7500	0.2500	0.5000	1959(14)
O(1)	0.9490(2)	0.1667(1)	0.5098(2)	2490(46)
O(2)	1.2460(2)	0.0400(1)	0.5028(2)	2869(47)
O(3)	0.8745(2)	0.3704(1)	0.3957(2)	3118(52)
O(4)	0.8200(2)	0.2895(1)	0.8004(2)	3419(52)
C(1)	0.9749(2)	0.0748(2)	0.5046(3)	1829(56)
C(2)	1.1114(2)	0.0178(1)	0.5020(3)	1885(57)

The complete temperature factor is $\exp(-8\pi^2 U_{\text{eq}} \sin^2 \theta / \lambda^2)$, where $U_{\text{eq}} = \frac{1}{3} \sum_{ij} U_{ij} a_i^* a_j^* \cdot a_i \cdot a_j$ in units of \AA^2 .

TABLE 3. Non-H-atom parameters and equivalent isotropic thermal parameters (\AA^2) with e.s.d.s in parentheses for the structure of $\text{Cu}(\text{C}_4\text{O}_4) \cdot 4\text{H}_2\text{O}$ (**2**)

Atom	x	y	z	$U_{\text{eq}} \times 10^4$
Cu	0.0000	0.0000	0.0000	177(2)
O(1)	0.3862(4)	0.0065(3)	0.1820(3)	235(7)
O(2)	0.5535(4)	0.2849(3)	0.5102(4)	330(10)
C(1)	0.4495(5)	0.0031(5)	0.3578(4)	183(9)
C(2)	0.5240(6)	0.1284(4)	0.5042(6)	196(11)
O(3)	-0.0060(4)	0.2467(3)	-0.0074(4)	331(9)
O(4)	-0.0772(4)	0.0074(3)	0.2226(3)	270(8)

The complete temperature factor is $\exp(-8\pi^2 U_{\text{eq}} \sin^2 \theta / \lambda^2)$, where $U_{\text{eq}} = \frac{1}{3} \sum_{ij} U_{ij} a_i^* a_j^* \cdot a_i \cdot a_j$ in units of \AA^2 .

$\text{Fe}(1)\text{--}\text{O}(4) = 2.106(2) \text{ \AA}$. The O-Fe-O angles deviate by less than 5° from 90.0° .

Compound **2** is not isostructural with **1** and the transition-metal squarate tetrahydrate series [1]. In **2**, copper(II) is coordinated to the p_π -orbital of the squarate oxygen (the torsion angle $\text{C}(2)\text{--}\text{C}(1)\text{--}\text{O}(1)\text{--}\text{Cu} = -100.2^\circ$). The geometry around copper(II) is characteristic of a Jahn-Teller distortion. The copper(II) to squarate oxygen bond length, $\text{Cu}\text{--}\text{O}(1) = 2.469(2) \text{ \AA}$, is much longer than the copper to water oxygen bond length, $\text{Cu}\text{--}\text{O}(3) = 1.961(3)$ and $\text{Cu}\text{--}\text{O}(4) = 1.98(2) \text{ \AA}$. The O-Cu-O angles deviate by less than 3° from 90° .

Stereo drawings of the packing pattern of **1** and **2** are given in Figs. 2 and 3, respectively. In the structure of **1**, the plane of the squarate anion and the plane formed by iron(II) and the water oxygen atoms are nearly perpendicular. In the structure of **2**, the plane of the squarate anion is nearly coplanar with the plane formed by the copper(II) and the water oxygen atoms. In both structures, the squarate anions stack in such a way that the distance between squarate anions is approximately $c/2$ in **1** and $a/2$ in **2**.

The squarate anion acts as a bidentate bridging ligand in **1** and **2**, the typical bonding mode for squaric acid with small transition metal ions [4]. This results in the

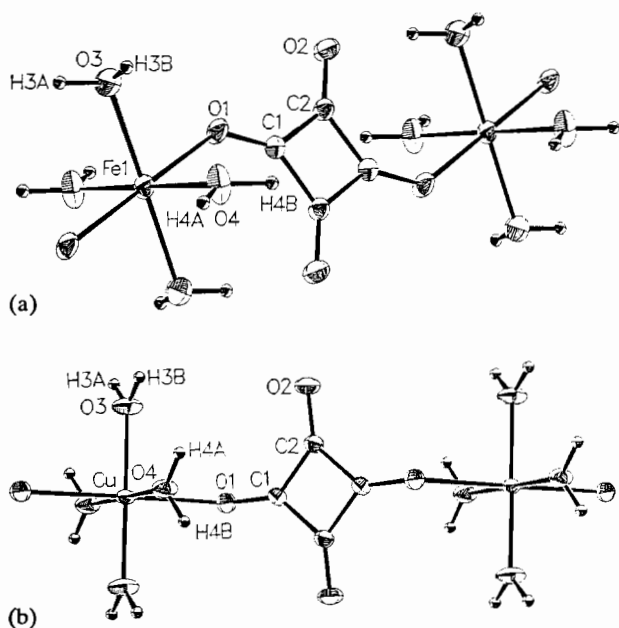


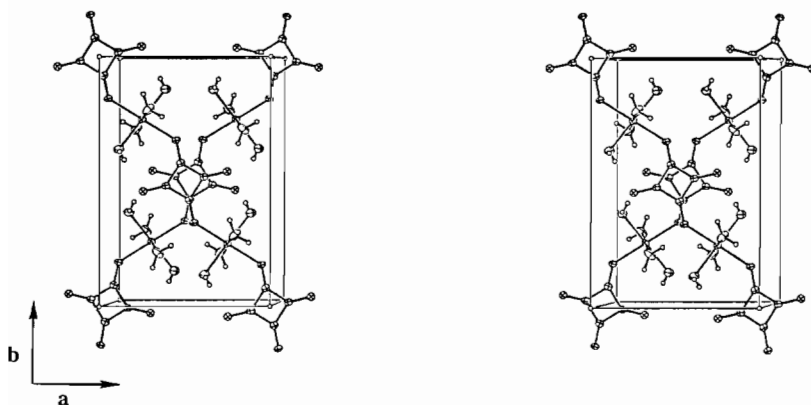
Fig. 1. Labeled ORTEP drawings of portions of the metal squarate chains (a) $\text{Fe}(\text{C}_4\text{O}_4) \cdot 4\text{H}_2\text{O}$ (**1**) and (b) $\text{Cu}(\text{C}_4\text{O}_4) \cdot 4\text{H}_2\text{O}$ (**2**).

TABLE 4. Bond lengths (Å) and bond angles (°) with e.s.d.s in parentheses for the structure of $\text{Fe}(\text{C}_4\text{O}_4) \cdot 4\text{H}_2\text{O}$ (1)

Interatomic distances (Å)					
Fe(1)–O(1)	2.115(2)	Fe(1)–O(3)	2.151(2)	Fe(1)–O(4)	2.106(2)
O(1)–C(1)	1.257(2)	O(2)–C(2)	1.255(3)	C(1)–C(2)	1.457(3)
Bond angles (°)					
O(1)–Fe(1)–O(3)	85.37(6)	O(1)–Fe(1)–O(3)	94.63(6)		
O(1)–Fe(1)–O(4)	91.56(6)	O(1)–Fe(1)–O(4)	88.44(6)		
O(3)–Fe(1)–O(4)	91.89(7)	O(3)–Fe(1)–O(4)	88.11(7)		
C(1)–O(1)–Fe(1)	132.8(1)	O(1)–Fe(1)–O(1)	180.0		
O(3)–Fe(1)–O(3)	180.0	O(4)–Fe(1)–O(4)	180.0		
O(1)–C(1)–C(2)	132.7(2)	O(1)–C(1)–C(2)	137.0(2)		
O(2)–C(2)–C(1)	135.7(2)	O(2)–C(2)–C(1)	134.6(2)		
C(2)–C(1)–C(2)	90.3(2)	C(1)–C(2)–C(1)	89.7(2)		

TABLE 5. Bond lengths (Å) and bond angles (°) with e.s.d.s in parentheses for the structure of $\text{Cu}(\text{C}_4\text{O}_4) \cdot 4\text{H}_2\text{O}$ (2)

Interatomic distances (Å)					
Cu–O(1)	2.469(2)	Cu–O(3)	1.961(3)	Cu–O(4)	1.948(2)
O(1)–C(1)	1.265(4)	O(2)–C(2)	1.257(4)	C(1)–C(2)	1.452(5)
Bond angles (°)					
O(4)–Cu–O(1)	92.68(9)	O(4)–Cu–O(1)	87.32(9)		
O(4)–Cu–O(3)	90.8(1)	O(4)–Cu–O(3)	89.2(1)		
O(3)–Cu–O(1)	90.2(1)	O(3)–Cu–O(1)	89.8(1)		
C(1)–O(1)–Cu	119.8(2)	O(1)–Cu–O(1)	180.0		
O(3)–Cu–O(3)	180.0	O(4)–Cu–O(4)	180.0		
C(2)–C(1)–C(2)	90.5(3)	O(1)–C(1)–C(2)	135.0(4)		
O(1)–C(1)–C(2)	134.6(4)	O(2)–C(2)–C(1)	135.5(4)		
O(2)–C(2)–C(1)	135.0(4)	C(1)–C(2)–C(1)	89.5(3)		

Fig. 2. Stereo drawings of the packing pattern of $\text{Fe}(\text{C}_4\text{O}_4) \cdot 4\text{H}_2\text{O}$ (1) projected onto the (110) plane.

formation of metal squarate chains where the chains in both structures are linked by intermolecular hydrogen bonds. In **1**, only the squarate oxygen atoms act as hydrogen-bond acceptors. In the structure of **1**, two hydrogen bonds link glide-related chains, one hydrogen bond links screw-related chains and the other one is intramolecular. Hydrogen-bond distances and angles for **1** are given in Table 6. In **2**, unlike **1**, only the water oxygen atoms act as hydrogen-bond acceptors. Two hydrogen bonds link the same screw-related chains,

and the other two hydrogen bonds link the same glide-related chains. Hydrogen-bond distances and angles for **2** are given in Table 7.

Our EHMO calculations indicate that there is a negligible overlap between the metal and the squarate orbitals in the HOMO and LUMO of the model clusters $[\text{Fe}(\text{OH})_4(\text{C}_4\text{O}_4)_2]^{6-}$ and $[\text{Cu}(\text{OH})_4(\text{C}_4\text{O}_4)_2]^{6-}$. This is due to the fact that the frontier orbitals of the squarate ion have large coefficients on the carbon atoms but small coefficients on the oxygen atoms. Furthermore,

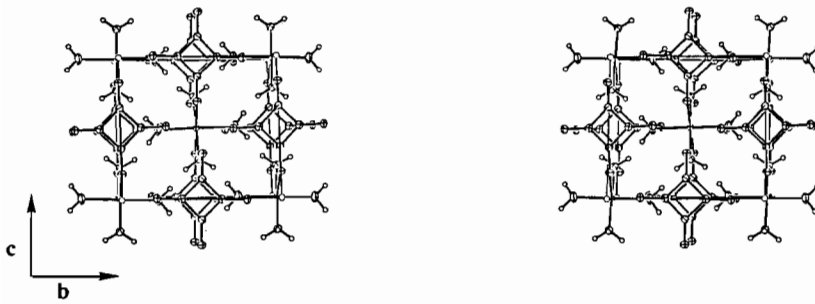


Fig. 3. Stereo drawings of the packing pattern of $\text{Cu}(\text{C}_4\text{O}_4)\cdot 4\text{H}_2\text{O}$ (2) projected onto the (011) plane.

TABLE 6. Hydrogen-bond lengths (\AA) and hydrogen-bond angles ($^\circ$) for the structure of $\text{Fe}(\text{C}_4\text{O}_4)\cdot 4\text{H}_2\text{O}$ (1)

Geometry of the hydrogen bonds linking the glide-related chains	
$\text{O}(2)\cdots\text{O}(3)$	2.99
$\text{O}(2)\cdots\text{H}(3\text{B})$	1.86
$\text{O}(3)\cdots\text{H}(3\text{B})$	0.89
$\text{O}(2)\cdots\text{H}(3\text{B})\text{---}\text{O}(3)$	151
$\text{O}(1)\cdots\text{O}(4)$	2.82
$\text{O}(1)\cdots\text{H}(4\text{A})$	1.92
$\text{O}(4)\cdots\text{H}(4\text{A})$	0.93
$\text{O}(1)\cdots\text{H}(4\text{A})\text{---}\text{O}(1)$	164
Geometry of the hydrogen bonds linking the screw-related chains	
$\text{O}(2)\cdots\text{O}(4)$	2.80
$\text{O}(2)\cdots\text{H}(4\text{B})$	1.86
$\text{O}(4)\cdots\text{H}(4\text{B})$	0.95
$\text{O}(2)\cdots\text{H}(4\text{B})\text{---}\text{O}(4)$	176
Geometry of the intramolecular hydrogen bond	
$\text{O}(2)\cdots\text{O}(3)$	2.71
$\text{O}(2)\cdots\text{H}(3\text{A})$	1.83
$\text{O}(3)\cdots\text{H}(3\text{A})$	0.90
$\text{O}(2)\cdots\text{H}(3\text{A})\text{---}\text{O}(3)$	166

TABLE 7. Hydrogen-bond lengths (\AA) and hydrogen-bond angles ($^\circ$) for the structure of $\text{Cu}(\text{C}_4\text{O}_4)\cdot 4\text{H}_2\text{O}$ (2)

Geometry of the hydrogen bonds linking the screw-related chains	
$\text{O}(3)\cdots\text{O}(4)$	2.92
$\text{O}(3)\cdots\text{H}(4\text{A})$	2.08
$\text{O}(4)\cdots\text{H}(4\text{A})$	0.89
$\text{O}(3)\cdots\text{H}(4\text{A})\text{---}\text{O}(4)$	158
$\text{O}(4)\cdots\text{H}(3\text{A})$	2.10
$\text{O}(3)\cdots\text{H}(3\text{A})$	0.92
$\text{O}(4)\cdots\text{H}(3\text{A})\text{---}\text{O}(3)$	148
Geometry of the hydrogen bonds linking the glide-related chains	
$\text{O}(3)\cdots\text{O}(4)$	2.77
$\text{O}(3)\cdots\text{H}(4\text{B})$	1.98
$\text{O}(4)\cdots\text{H}(4\text{B})$	0.85
$\text{O}(3)\cdots\text{H}(4\text{B})\text{---}\text{O}(4)$	155
$\text{O}(4)\cdots\text{H}(3\text{B})$	1.98
$\text{O}(3)\cdots\text{H}(3\text{B})$	1.02
$\text{O}(4)\cdots\text{H}(3\text{B})\text{---}\text{O}(3)$	131

these calculations show that there is practically no stability difference between the p_σ - and the p_π -coordination modes of the squarate ion ligands in

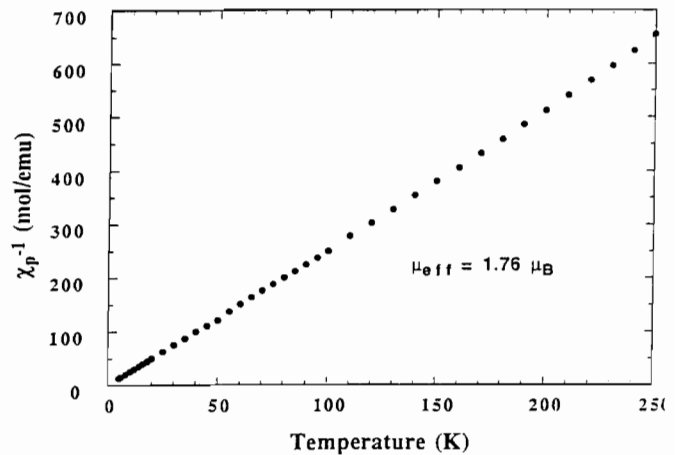


Fig. 4. The inverse of the corrected molar susceptibility, $1/\chi_p$, graphed as a function of temperature ($H=500$ Oe).

$[\text{Fe}(\text{OH})_4(\text{C}_4\text{O}_4)_2]^{6-}$, and that the p_π -coordination mode is slightly more stable than the p_σ -coordination mode in $[\text{Cu}(\text{OH})_4(\text{C}_4\text{O}_4)_2]^{6-}$ (by about 3.7 kcal mol $^{-1}$).

After applying the diamagnetic correction to the molar susceptibility of the copper(II) ion in 2 ($\chi_D = -12.8 \times 10^{-6}$ cm 3 mol $^{-1}$), the inverse of the corrected molar susceptibility, $1/\chi_p$, was plotted as a function of temperature in Fig. 4. The effective magnetic moment, $\mu_{\text{eff}} = 1.76 \pm 0.15$ emu, was calculated from the slope of $1/\chi_p$ versus T . The linear relationship between $1/\chi_p$ and T indicates that the temperature independent susceptibility, χ_o , is negligible. The x intercept of this plot, i.e. the Weiss constant θ , is -4.1 K. This small value is consistent with the absence of long range ordering of the copper(II) ion moments.

Discussion

Partial oxidation or reduction of the metal sites in 1 and 2 was planned as a route to producing polymeric conductors. However, EHMO calculations have revealed that 1 and 2 are not good candidates for conversion to polymeric electrical conductors because mixing of the metal orbitals and the squarate oxygen orbitals is negligible in the HOMO and LUMO of $[\text{Fe}(\text{OH})_4(\text{C}_4\text{O}_4)_2]^{6-}$ or $[\text{Cu}(\text{OH})_4(\text{C}_4\text{O}_4)_2]^{6-}$. This in-

dicates that conduction of electrons through the iron(II) and copper(II) squarate chains is unlikely.

By use of EHMO calculations, the p_{π} -coordination of the copper(II) ion to the squarate oxygen in $[\text{Cu}(\text{OH})_4(\text{C}_4\text{O}_4)_2]^{6-}$ was found to be slightly more stable than the p_{σ} -coordination mode. This calculated stability difference is consistent with the structures of **2** and $\text{Cu}(\text{C}_4\text{O}_4) \cdot 2\text{H}_2\text{O}^*$, but it is a small difference and may not be significant. Most likely, packing requirements associated with the ligands and the interligand hydrogen bonding are largely responsible for directing the coordination modes of the metal(II) ions to the squarate oxygen atoms in **1** and **2**.

Compound **2** follows Curie–Weiss behavior with a correlation coefficient of 0.9998 for $1/\chi_p$ versus T (Fig. 4). The effective magnetic moment of **2**, $\mu_{\text{eff}} = 1.76 \pm 0.15$ emu, indicates that each copper(II) has a localized electron. It is of interest to note that the HOMO of $[\text{Cu}(\text{OH})_4(\text{C}_4\text{O}_4)_2]^{6-}$, which is half filled, is the x^2-y^2 block orbital whose d-orbital has a δ -type symmetry along the axis toward the oxygen atoms of the squarate ligands. Thus, the orbitals of the squarate ligands do not mix into the HOMO. Consequently, the radical-containing orbitals of **2** are not expected to interact via the squarate ligand bridges. Thus, **2** should behave as a paramagnetic system, in agreement with magnetic measurements.

Conclusions

The present EHMO calculations show that **1** and **2** are not expected to be good candidates for polymeric electrical conductors. These calculations also suggest that electronic forces are not responsible for the orientation of copper(II) towards the p_{π} -orbital of the oxygen in **2**. Differences in structural arrangements of **1** and **2** must be due to packing forces associated with hydrogen bonding and Jahn–Teller distortion in **2**. The change in packing forces in these molecularly similar compounds may stem from the Jahn–Teller distortion of the copper(II) in **2**. The effective magnetic moment of **2**, $\mu_{\text{eff}} = 1.76 \pm 0.15$ emu, derived from magnetic measurements, is very close to the theoretical spin-only moment of copper(II) (i.e. 1.73 mB). The symmetry of the crystal field at the copper site is so low that the

orbital moment is completely quenched. The results of the magnetic measurements are consistent with predictions from EHMO calculations on the model compound of **2**.

Acknowledgements

This work was supported by the US Department of Energy, Office of Basic Energy Sciences, Division of Materials Science under Contract W-31-109-ENG-38; the National Science Foundation, Office of Science and Technology Centers under Contract STC8809854; and the US Department of Energy, Office of Basic Energy Sciences, Division of Materials Sciences, under Grant DE-FG05-86ER45249. The authors thank Dr Lynda Soderholm, Argonne National Laboratory, for helpful discussions, and Dr O. Eisenstein for invaluable comments.

References

- 1 A. Weiss, E. Riegler, I. Alt. H. Böhme and C. Robl, *Z. Naturforsch., Teil B*, **41** (1986) 18.
- 2 J.-C. Trombe, J.-F. Petit and A. Gleizes, *New J. Chem.*, **12** (1988) 197.
- 3 (a) J. P. Collman, J. T. McDevitt, G. T. Yee, C. R. Leidner, L. G. McCullough, W. A. Little and J. B. Torrance, *Proc. Natl. Acad. Sci. U.S.A.*, **83** (1986) 4581; (b) J. P. Collman, J. T. McDevitt, C. R. Leidner, G. T. Yee, J. B. Torrance and W. A. Little, *J. Am. Chem. Soc.*, **109** (1987) 4606.
- 4 C. P. Poole, T. Datta and H. A. Farach, *Copper Oxide Superconductors*, Wiley, New York, 1988.
- 5 R. Hoffmann, *J. Chem. Phys.*, **39** (1963) 1397.
- 6 (a) T. A. Albright, J. K. Burdett and M.-H. Whangbo, *Orbital Interactions in Chemistry*, Wiley, New York, 1985, Ch. 13; (b) M.-H. Whangbo, in J. Rouxel (ed.), *Crystal Chemistry and Properties of Materials with Quasi-One-Dimensional Structures*, Reidel, Boston, MA, 1986, p. 205.
- 7 D. Semmingsen, *Acta Scand.*, **27** (1973) 3961.
- 8 (a) G. C. Gerstein and M. Habenschuss, *J. Appl. Phys.*, **43** (1972) 5155; (b) M. Habenschuss and B. C. Gerstein, *J. Chem. Phys.*, **61** (1974) 852.
- 9 P. Main, S. E. Hull, L. Lessinger, G. Germain, J.-P. Declercq and M. M. Woolfson, *MULTAN78*, a system of computer programs for the automatic solution of crystal structures from X-ray diffraction data, Universities of York, UK, and Louvain, Belgium, 1978.
- 10 *International Tables for X-ray Crystallography*, Vol. IV, Kynoch, Birmingham, UK, 1974 (Present distributor D. Reidel, Dordrecht).
- 11 C. Strouse, *UCLA Crystallographic Package*, University of California, Los Angeles, CA, 1978.
- 12 C. Robl and A. Weiss, *Z. Naturforsch., Teil B*, **41** (1986) 1341.

*Coordination of the copper(II) to the squarate oxygen atom is also found in the structure of $\text{Cu}(\text{C}_4\text{O}_4) \cdot 2\text{H}_2\text{O}$ [12].